MULTICHANNEL GUIDED IMAGE FILTER

Chang Liu[†], *Xiaolin Wu*[†‡], *Xiao Shu*[†‡]

† Shanghai Jiao Tong University
‡ McMaster University

ABSTRACT

Guided image filter (GIF) is an edge-preserving filtering technique that smooths the fine texture of an input image with the guide of a second image. One shortcoming of GIF and all its existing variants, such as, weighed guided image filter and gradient domain guided image filter, is that they only use one grayscale image as the guide and are consequently unable to fully utilize the rich information offered by multichannel images. In this paper, we extend GIF for multichannel guidance image and propose a novel correlation detection technique for retaining sharp edges with opposite gradient directions in the different channels of the same guidance image. Experimental results show that the proposed method preserves the details from both the input and guidance images better than existing GIF techniques.

Index Terms— Edge-preserving, guided image filter, multichannel.

1. INTRODUCTION

Edge-preserving smoothing refers to a group of image processing techniques that smooth image detail without adversely affecting the sharpness of edges. These techniques have been widely adopted in various applications, including image fusion [1, 2], image demising [3, 4], high dynamic range tone mapping [5], image detail enhancement [6], image stitching [7] and haze removal [8].

Existing edge-preserving smoothing techniques can be broadly classified into two categories: global optimization based and local filtering based. Global optimization based techniques, such as total variation [4, 9, 10], weighted least square [11, 12] and $L0$-norm gradient minimization [13], find the best output image by solving an optimization problem regularized by fidelity and smoothness terms. These global optimization based techniques can produce high quality results but are computationally expensive and unsuitable for real-time applications. In contrast, local filtering based techniques, such as bilateral filter [14, 15, 5, 16, 17], trilateral filter [18] and guided image filter (GIF) [19], require much shorter run-time but are prone to various artifacts like halo and gradient reversal.

Among all the edge-preserving smoothing techniques, local filtering method GIF is one of the fastest. GIF is based on the idea of linearly transforming a second image, called guidance image, to match the input image in each window. A smoothed version of the input image is then reconstructed using the transform coefficients. In comparison to other local filtering methods, GIF is less subject to gradient reversal artifacts. Its major weakness in causing halo and blurring edges is lessened in the latest variants of GIF such as weighted guided image filter (WGIF) [20] and gradient domain guided image filter (GDGIF) [21].

In this paper, we propose a further improvement to GIF, namely, multichannel guided image filter (MGIF). One limitation of the existing GIF methods is that the guidance image must be a single grayscale image; only the luminance channel is utilized if the guidance image is in color. Discarding the extra channels in the guidance image removes many perceivable edge details, reducing the effectiveness of GIF in retaining edges. However, it is a challenging task to fully take the advantage of a multichannel guidance image. For instance, the same edge of different channels in a guidance image may have exact opposite gradient directions, potentially canceling each other during the design of the guided filter. To alleviate this problem, we introduce a correlation detection algorithm for detecting the gradient direction of an edge in every channel. With this information of edge direction, the linear transform coefficients in each channel can be designed accordingly to prevent the objectionable cancellation effects. By exploiting the extra information from the different channels of the guidance image, the proposed MGIF is highly reliable in preserving image edges.

The rest of the paper is organized as follows. Section 2 presents the detail of MGIF and Section 3 analyzes its theoretical properties. Section 4 evaluates MGIF and compares it against other methods. Finally, Section 5 concludes the paper.

2. MULTICHANNEL GUIDED IMAGE FILTER

The proposed method is inspired by the very effective edge-preserving smoothing technique GIF [19]. In GIF, an input image X is filtered based on the features of a second image I, called the guidance image. The basic idea of GIF is to let the smoothed output image Y be a linear transform of guidance

image I in each window $\Omega(k)$ centered at pixel k, i.e.,

$$Y(i) \approx a_k I(i) + b_k, \quad \forall i \in \Omega(k). \tag{1}$$

where scalars a_k, b_k are the linear transform coefficients decided by the relationship between guidance image I and input image X in that window. To obtain a_k, b_k for each window, GIF minimizes a cost function H_k defined as,

$$H_k = \sum_{i \in \Omega(k)} \left[(a_k I(i) + b_k - X(i))^2 + \lambda a_k^2 \right], \tag{2}$$

where λ is a regularization parameter controlling penalizing term for large a_k. This minimization problem in Eq. (2) is a linear ridge regression problem, which has a closed form solution as follows,

$$\begin{aligned} a_k &= \frac{\tilde{\mu}_{I \circ X}(k) - \tilde{\mu}_I(k)\tilde{\mu}_X(k)}{\sigma_I^2(k) + \lambda}, \\ b_k &= \tilde{\mu}_X(k) - a_k \tilde{\mu}_I(k), \end{aligned} \tag{3}$$

where $I \circ X$ is the entry-wise product of I and X; and $\tilde{\mu}_{I \circ X}(k)$, $\tilde{\mu}_I(k)$ and $\tilde{\mu}_X(k)$ are the mean value of $I \circ X$, I and X in window $\Omega(k)$, respectively.

Although GIF and its variants, such as, WGIF [20] and GDGIF [21], have many nice properties in retaining sharp edges and preventing various artifacts, they lack the capability in fully utilizing multichannel guidance image for better edge preservation as discussed previously. To solve this problem, we formulate our MGIF based on the latest variant GDGIF. For the sake of simplicity in the formulation, we use I_0 to denote the input image and name each of the m channels in the guidance image as $I_1, I_2, ..., I_m$, respectively. Then, directly derived from the GDGIF as in [21], the new cost function can be written as,

$$\begin{aligned} H_k = \sum_{i \in \Omega(k)} [(\sum_{j=1}^{m} a_{kj} I_j(i) + b_k - I_0(i))^2 \\ + \sum_{j=1}^{m} w_{kj} (a_{kj} - \widehat{\gamma}_{kj})^2], \end{aligned} \tag{4}$$

where a_{kj} is the linear coefficients of the j-th guidance image channel I_j and w_{kj} is the edge-aware weight of I_j. In general, for the best result of edge preservation, weight w_{kj} should be less than 1 if pixel k is on an edge, and greater than 1 if pixel k is in a smooth area [20]. Since there are multiple channels in the guidance image, the weighting should consider not only the content within each channel but also the content of the same location among different channels. With both factors being taken into account, we define the edge-aware weight w_{kj} for the proposed MGIF using local variances $\sigma_j^2(k)$ of window $\Omega(k)$ as follows,

$$w_{kj} = \frac{\lambda_1 \operatorname{E}_k[\sigma_j^2(k)] + \lambda_2 \operatorname{E}_j[\sigma_j^2(k)]}{\sigma_j^2(k) + \varepsilon}, \tag{5}$$

where $\operatorname{E}_k[\sigma_j^2(k)]$ is the mean value of local variances $\sigma_j^2(k)$ of all pixels in j-th guidance image channel, and $\operatorname{E}_j[\sigma_j^2(k)]$ is the mean value of local variances $\sigma_j^2(k)$ at pixel k in all guidance image channels. Constants λ_1, λ_2 are two regularization parameters, and $\varepsilon = (0.001L)^2$ with L being the number of graylevels of the input image is a small constant added to the denominator to prevent division by 0. The weight w_{jk} defined in Eq. (5) is a comprehensive measure of the importance of pixel k in I_j with respect to the whole pixels in I_j and the importance of pixel k in among all guidance image channels.

Another important constant in Eq. (4) is the explicit first-order edge-aware constraint parameter γ_{kj}. For the best result, parameter γ_{kj} should approach 1 if pixel k is on an edge, and approach 0 if k is in a smooth area [21]. This parameter is designed to bias a_{kj} to 1 or 0 based on whether pixel k is on an edge, making the proposed filter less sensitive to the selection of λ_1 and λ_2. By using a negative power function, we define γ_{kj} as,

$$\gamma_{kj} = \frac{2}{1 + e^{-t}} - 1, \tag{6}$$

where $t = \sigma_j^2(k) / \operatorname{E}_k[\sigma_j^2(k)]$. As designed, the parameter increases monotonically with variance $\sigma_j^2(k)$; the value of γ_{kj} approaches 0 for small $\sigma_j^2(k)$ and approaches 1 for large $\sigma_j^2(k)$.

Unlike the previous work in [21], MGIF utilizes more than one channels as guide. The information from multiple channels can lead to a new problem of mutual interference, since a window at some location may have conflict properties in different channels. For example, the transition of an edge can be convex in one channel and concave in another channel. To solve the problem, we can detect the correlation of guidance image and input image. Suppose that $\mu_{j0}(k)$, $\mu_j(k)$ and $\mu_0(k)$ are the mean value of $I_j \circ I_0$, I_j and I_0 in the window $\Omega(k)$. Then, the local covariance of guidance image channel I_j and input image I_0 at pixel k is defined as,

$$cov_{j0}(k) = \mu_{j0}(k) - \mu_j(k)\mu_0(k). \tag{7}$$

If the covariance function is positive, then the gradient direction of the j_{th} guidance image I_j and the input image I_0 is the same, and the value of γ_{kj} should be positive; if the covariance function is negative, then the gradient direction of the j_{th} guidance image I_j and the input image I_0 is reversed, and the value of γ_{kj} should be negative. Based on the covariance function in Eq. (7), we define a new first-order edge-aware constraint parameter $\widehat{\gamma}_{kj}$ that is invariant to the gradient direction of an edge as,

$$\widehat{\gamma}_{kj} = \operatorname{sgn}(cov_{j0}(k)) \cdot \gamma_{kj}, \tag{8}$$

where $\operatorname{sgn}(x)$ is a sign function with output value being 1 if $x \geq 0$ and -1 if $x < 0$.

Now we can calculate the value of w_{kj} by Eq. (5) and $\widehat{\lambda}_{kj}$ by Eqs. (6), (7) and (8). The optimal value of a_{kj} and b_k can

then be obtained by minimizing the cost function in Eq. (4) as follows,

$$A_k = (\mathbf{C}_{j_1 j_2} + \mathbf{W})^{-1}(C_{j0} + \Psi),$$
$$b_k = \mu_0(k) - \sum_{j=1}^{m} a_{kj}\mu_j(k), \tag{9}$$

where,

$$A_k = \begin{bmatrix} a_{k1} & a_{k2} & ... & a_{km} \end{bmatrix}^\top,$$
$$\mathbf{C}_{j_1 j_2} = \begin{bmatrix} cov_{11}(k) & cov_{21}(k) & \cdots & cov_{m1}(k) \\ cov_{12}(k) & cov_{22}(k) & \cdots & cov_{m2}(k) \\ \vdots & \vdots & \ddots & \vdots \\ cov_{1m}(k) & cov_{2m}(k) & \cdots & cov_{mm}(k) \end{bmatrix},$$
$$\mathbf{W} = \mathrm{diag}(w_{k1}, w_{k2}, \ldots, w_{km}),$$
$$C_{j0} = \begin{bmatrix} cov_{10}(k) & cov_{20}(k) & \cdots & cov_{m0}(k) \end{bmatrix}^\top,$$
$$\Psi = \begin{bmatrix} w_{k1}\widehat{\gamma}_{k1} & w_{k2}\widehat{\gamma}_{k2} & \cdots & w_{km}\widehat{\gamma}_{km} \end{bmatrix}^\top. \tag{10}$$

Finally, the output image Y can be computed as

$$Y(k) = \sum_{j=1}^{m} \overline{a_{kj}} I_j(k) + \overline{b_k}, \tag{11}$$

where $\overline{a_{kj}}$ and $\overline{b_k}$ are the mean values of a_{kj} and b_k in the window $\Omega(k)$, respectively. Since for each pixel, the most time consuming step of this algorithm is to find the inverse matrix of $\mathbf{C}_{j_1 j_2} + \mathbf{W}$, the overall time complexity for filtering a m-channel and N-pixel image is $O(N \cdot f(m))$, where $f(m)$ is the time cost for inverting a $m \times m$ matrix.

3. MULTICHANNEL EDGE PRESERVATION

After giving the definition of multichannel guided image filter, we can analyze its edge-preserving property. First, assume that the guidance image has two channels, where the first channel I_1 is the same as input image I_0, and the second one I_2 is the negative of the input image I_0. Thus, $\sigma_1^2(k) = \sigma_2^2(k) = -cov_{12}(k)$ and $w_{k1} = w_{k2}$. Now let us consider two cases.

Case 1: pixel k is on an edge, the values of $\widehat{\gamma}_{k1}$ is close to 1, the value of $\widehat{\gamma}_{k2}$ is close to -1. Therefore, coefficients a_{k1}, a_{k2} are,

$$a_{k1} = \frac{\sigma_1^2(k) + w_{k1}}{2\sigma_1^2(k) + w_{k1}},$$
$$a_{k2} = -\frac{\sigma_1^2(k) + w_{k1}}{2\sigma_1^2(k) + w_{k1}}. \tag{12}$$

As pixel k is on an edge, $\sigma_1^2(k)$ is large, we have $\sigma_1^2(k) \gg w_{k1}$, so a_{k1}, a_{k2} are $1/2$,$-1/2$, respectively, regardless of the value of $\lambda 1$ and $\lambda 2$. Here, a_{k1} is positive due to the positive correlation between I_1 and I_0, and a_{k2} is negative due to the negative correlation between I_2 and I_0.

Case2: pixel k is in a smooth area, the values of $\widehat{\gamma}_{k1}$ and $\widehat{\gamma}_{k2}$ are both close to 0. Therefore, coefficients a_{k1}, a_{k2} are,

$$a_{k1} = \frac{\sigma_1^2(k)}{2\sigma_1^2(k) + w_{k1}}, \tag{13}$$
$$a_{k2} = -\frac{\sigma_1^2(k)}{2\sigma_1^2(k) + w_{k1}}. \tag{14}$$

As pixel k is in a smooth area, $\sigma_1^2(k)$ is close to 0, and a_{k1}, a_{k2} are both close to 0 as well.

Now we analyze the effect of correlation detection in $\widehat{\gamma}_{kj}$. Assume that the guidance image has two channels and both channels are the negative of the input image I_0. Then $\sigma_1^2(k) = \sigma_0^2(k) = -cov_{10}(k)$ and $w_{k1} = w_{k2}$. If the pixel k is on an edge, then $\widehat{\gamma}_{k1}$ and $\widehat{\gamma}_{k2}$ are both close to -1. Similar to the previous discussion, we can get coefficients a_{k1}, a_{k2} as

$$a_{k1} = a_{k2} = -\frac{\sigma_1^2(k) + w_{k1}}{2\sigma_1^2(k) + w_{k1}}. \tag{15}$$

However, if we do not employ the correlation detection technique and use γ_{kj} from Eq. (6) to calculate coefficients a_{k1}, a_{k2}, the result is

$$a_{k1} = a_{k2} = -\frac{\sigma_1^2(k) - w_{k1}}{2\sigma_1^2(k) + w_{k1}}, \tag{16}$$

since both γ_{k1}, γ_{k2} are close to 1. In comparison with Eq. (16), the resulting value of a_{k1}, a_{k2} by Eq. (15) is closer to $-1/2$, implying that the edge is preserved better in the previous case where γ_{kj} is obtained with correlation detection using Eq. (8).

4. EXPERIMENTAL RESULTS

To evaluate the performance of MGIF, we implement the algorithm in Matlab and compare its results against the results from GIF and GDGIF for image fusion. The problem of image fusion is to merge several images into one image which preserves all the details from each input image. Shown in Fig. 1 is an example of image fusion between a visible light image (Fig. 1a) and an infrared image (Fig. 1b). Each of the infrared and visible light images has some unique details. For example, the contours of the liquid soap bottle and headset only have good contrast in the infrared image, while the label of the soap bottle is only perceivable in the visual light image. The problem is to make these details from different channels reinforce rather than cancel each other in the output image. We tested GDGIF in two configurations for the pair of test images. In the first configuration, GDGIF takes the visible light image as the input and infrared image as the guide. As shown in Fig. 1c, the details from the infrared image, such as the edge, are well transferred in this output image. But

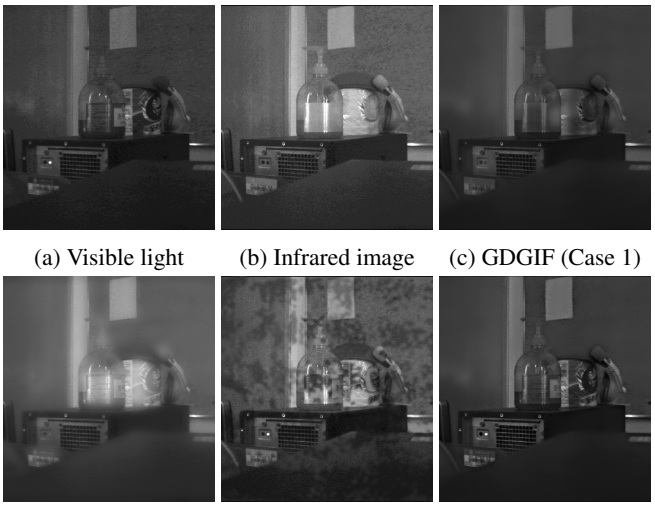

(a) Visible light (b) Infrared image (c) GDGIF (Case 1)

(d) GDGIF (Case 2) (e) GFF (f) MGIF

Fig. 1: Examples of image fusion. Parameter $\lambda = 0.2^2$ for GIF and GDGIF, $\lambda_1 = \lambda_2 = 0.2^2$ for the proposed MGIF.

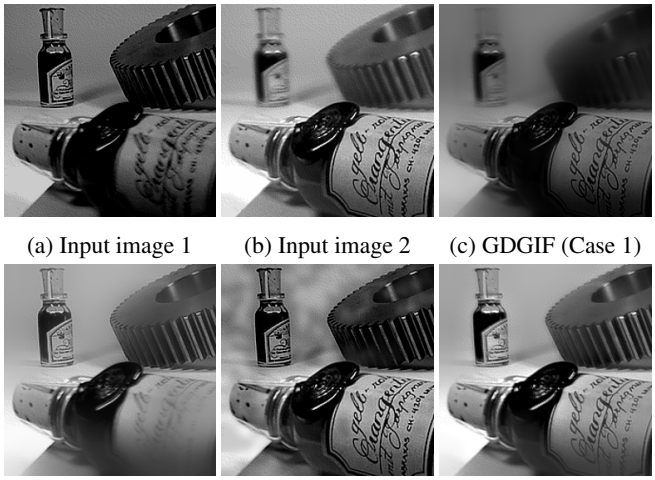

(a) Input image 1 (b) Input image 2 (c) GDGIF (Case 1)

(d) GDGIF (Case 2) (e) GFF (f) MGIF

Fig. 2: Examples of image fusion. Parameter $\lambda = 0.2^2$ for GIF and GDGIF, $\lambda_1 = \lambda_2 = 0.2^2$ for the proposed MGIF.

	LP [22]	DTCWT [23]	GFF [2]	LP-SR [24]	GTF [25]	MGIF
SD	39.1049	35.4248	38.4276	**44.2431**	42.0855	43.0108
EN	6.7941	6.6796	6.7943	**6.9754**	6.4994	6.1968
MI	2.7450	2.5305	3.4128	3.1779	2.5203	**4.7507**

Table 1: Quantitative comparisons of MGIF with state-of-the-art image fusion algorithms. SD, EN and MI are abbreviations of standard deviation, entropy and mutual information, respectively.

some details, such as the labels, that are only visible in the input image (the visible light image) are missing in the output image. When we reverse the roles of the visible light and infrared images, and use visible light image as the guide, the result of GDGIF still has the same problem: some details, like the edge of the bottle, in the input image (the infrared image in this case) are not transferred to the output image as shown in Fig. 1d. Fig. 1e shows the result of guided filtering based fusion (GFF) [2]. This technique decomposes an image into a base layer and a detail layer and constructs the output image with a weighted sum of these two layers. Although the result of this method retains most of the details, it is plagued by artifacts due to the luminance difference between the guide and input. In comparison, as shown in Fig. 1f, the proposed MGIF is free of these problems. In this test for MGIF, the input image is the visible light image and the guidance image contains both the visible light and infrared channels. As MGIF exploits the details in both channels, it does not only preserve all the edges from both channels, it also greatly reduces the noise.

Fig. 2 shows another example of image fusion. In this case, the two input images capture the same scene but with different focal distances, thus, as shown in the figure, some parts of each image are in focus while other parts are blurred. None of the GDGIF or GIF methods can successfully combine all the sharp edges from both input images without producing objectionable artifacts. Compared to the other tested techniques, the proposed MGIF produce visually pleasing output image by fusing the sharp parts from two channels together. The resulting image is very close to an all-focused image.

In addition to subjective evaluation, we also compare the quantitative performance of MGIF against several state-of-the-art image fusion algorithms, including Laplacian pyranmid (LP) [22], dual-tree complex wavelet transform (DTCWT) [23], guided filtering based fusion (GFF) [2], Laplacian pyramid with sparse representation (LP-SR) [24], and gradient transfer and total variation minimization image fusion (GTF) [25], using the visible light and infrared image pairs from TNO image fusion dataset [29]. As shown in Table 1, the proposed MGIF is ranked among the top of the tested algorithms by most objective assessment measures, especially mutual information (MI) [28], which is specifically designed for assessing quality of image fusion.

5. CONCLUSION

In this paper, we extend the state-of-the-art GIF to support multichannel guidance image. In order to fully exploiting the extra information provided by a multichannel guidance image, we also propose a correlation detection technique for retaining sharp edges with opposite gradient directions in the different channels. Experimental results show that the proposed method preserves the details from both the input and guidance images better than existing GIF techniques.

6. REFERENCES

[1] J. H. Zheng Z. G. Li and S. Fatemi, "Detail-enhancement exposure fusion," *IEEE Trans. Image Process*, vol. 21, pp. 4672–4676, 2012.

[2] X. D. Kang S. T. Li and J. W. Hu, "Image fusion with guided filtering," *IEEE Trans. Image Process*, vol. 22, no. 7, pp. 2864, 2013.

[3] P. Charbonnier, "Deterministic edge-preserving regularization in computed imaging," *IEEE Trans. Image Process*, vol. 6, no. 2, pp. 298–311, 1996.

[4] S. Osher LI. Rudin and E. Fatemi, "Nonlinear total variation based noise removal algorithms," *Phys. D Nonlinear Phenomena*, vol. 60, no. 1-4, pp. 259–268, 1992.

[5] F. Durand and J. Dorsey, "Fast bilateral filtering for the display of high-dynamic-range images," *ACM Trans. Graph*, vol. 21, no. 3, pp. 257–266, 2002.

[6] M. Agrawala R. Fattal and S. Rusinkiewicz, "Multiscale shape and detail enhancement from multi-light image collections," *ACM Trans. Graph*, vol. 26, no. 3, pp. 2007, 2007.

[7] M. Gangnet P. Prez and A. Blake, "Poisson image editing," *ACM Trans. Graph*, vol. 22, no. 3, pp. 313–318, 2003.

[8] J. Sun K. He and X. Tang, "Single image haze removal using dark channel prior.," *IEEE Trans. Pattern Anal. Mach. Intell.*, vol. 33, no. 12, pp. 2341–53, 2011.

[9] Y. Xia L. Xu, Q. Yan and J. Jia, "Structure extraction from texture via relative total variation," *ACM Trans. Graph*, vol. 31, no. 6, pp. 139, 2012.

[10] O. V. Michailovich, "An iterative shrinkage approach to total-variation image restoration.," *IEEE Trans. Image Process*, vol. 20, no. 5, pp. 1281–1299, 2009.

[11] R. Fattal Z. Farbman and D. Lischinski, "Edge-preserving decompositions for multi-scale tone and detail manipulation," *ACM Trans. Graph*, vol. 27, no. 3, pp. 1–10, 2008.

[12] J. Lu D. Min, S. Choi and B. Ham, "Fast global image smoothing based on weighted least squares," *IEEE Trans. Image Process*, vol. 23, no. 12, pp. 5638, 2014.

[13] Y. Xu L. Xu, C. Lu and J. Jia, "Image smoothing via l0 gradient minimization," *ACM Trans. Graph*, vol. 30, no. 6, 2011.

[14] C. Tomasi and R. Manduchi, "Bilateral filtering for gray and color images," in *proc. 6th Int. Conf. Comput. Vis.(ICCV)*. IEEE, 1998, pp. 839–846.

[15] L. Xu Q. Zhang, X. Shen and J. Jia, "Rolling guidance filter," in *Eur. Conf. Comput. Vis.(ECCV)*. Springer, 2014, pp. 815–830.

[16] S. Paris and F. Durand, "A fast approximation of the bilateral filter using a signal processing approach," in *proc. 9th Eur. Conf. Comput. Vis.(ECCV)*. Springer, 2006, pp. 568–580.

[17] F. Porikli, "Constant time o (1) bilateral filtering," in *IEEE. Conf. Comput. Vis. and Pattern Recognit.(CVPR)*. IEEE, 2008, pp. 1–8.

[18] P. Choudhury and J. Tumblin, "The trilateral filter for high contrast images and meshes," in *ACM SIGGRAPH 2005 Courses*. ACM, 2005, p. 5.

[19] J. Sun K. He and X. Tang, "Guided image filtering," *IEEE Trans. Pattern Anal. Mach. Intell.*, vol. 35, no. 6, pp. 1397–1409, 2013.

[20] J. Zheng Z. Li and Z. Zhu et al., "Weighted guided image filtering," *IEEE Trans. Image Process*, vol. 24, no. 1, pp. 120–129, 2015.

[21] C. Wen F. Kou, W. Chen and Z. Li, "Gradient domain guided image filtering," *IEEE Trans. Image Process*, vol. 24, no. 11, pp. 4528–4539, 2015.

[22] E.H. Adelson P.J. Burt, "The laplacian pyramid as a compact image code," *IEEE Trans. Commun*, vol. 31, pp. 532–540, 1983.

[23] S.G. Nikolov D.R. Bull N. Canagarajah J.J. Lewis, R.J. OCallaghan, "Pixel-and region-based image fusion with complex wavelets," *Information Fusion*, vol. 8, pp. 119–130, 2007.

[24] Z. Wang Y. Liu, S. Liu, "A general framework for image fusion based on multi-scale transform and sparse representation," *Information Fusion*, vol. 24, pp. 147–164, 2015.

[25] C. Li J. Ma, C. Chen and J. Huang, "Infrared and visible image fusion via gradient transfer and total variation minimization," *Information Fusion*, vol. 31, pp. 100–109, Sep 2016.

[26] S. Baronti L. Alparone F. Nencini, A. Garzelli, "Remote sensing image fusion using the curvelet transform," *Def. Sci. J.*, vol. 61, pp. 479–484, 2011.

[27] V. Naidu, "Image fusion technique using multi-resolution singular value decomposition," *Information Fusion*, vol. 8, pp. 143–156, 2007.

[28] P. Yan G. Qu, D. Zhang, "Information measure for performance of image fusion," *Electron. Lett.*, vol. 38, pp. 313–315, 2002.

[29] Alexander Toet and Maarten A Hogervorst, "Progress in color night vision," *Optical Engineering*, vol. 51, no. 1, pp. 010901–010901, 2012.